Hindawi
Wireless Communications and Mobile Computing
Volume 2022, Article ID 8021862, 7 pages
https://doi.org/10.1155/2022/8021862

Research Article

Streak Metal Artifact Reduction Based on Sinogram Fusion and Tissue-Class Model in CT Images

Shuwen Deng,[1] Yuanjin Li,[2] and Dianhua Wang[1]

[1]*Computer Department, Hubei University of Science and Technology, Xianning 437100, China*
[2]*Computer Department, Chuzhou University, Chuzhou 239000, China*

Correspondence should be addressed to Yuanjin Li; liyuanjin@chzu.edu.cn

Received 3 March 2022; Revised 1 April 2022; Accepted 5 April 2022; Published 30 April 2022

Academic Editor: Kuruva Lakshmanna

The presence of streak metal artifacts seriously degrades the diagnostic value and deteriorates the qualities of CT images. Analyzing the causes and classical streak metal artifact reduction (MAR) methods, the paper proposes the streak metal artifact reduction method based on sinogram fusion and tissue-class mode for CT images (F-MAR). Firstly, the original CT images are corrected using a linear interpolation streak metal artifact reduction (L-MAR) scheme in the raw data domain. Subsequently, to preserve the edge information, the metal artifact-reduced images are then smoothed into smoothed images (tissue-class model) by using the mean filter. Segment the original CT image that contained the streak artifacts. The original CT image and the CT image that contained high-density material are projected into the original sinogram and the high density material sinogram, respectively. Secondly, the simple linear interpolation is used to correct the CT original CT image into the corrected CT image. The mean filter is applied in the corrected CT image. The corrected CT image is projected into the corrected sinogram. Thirdly, according to the position of the high density material sinogram located in the original sinogram and the corrected sinogram, the original position sinogram included in the original sinogram and the corrected position sinogram included in the corrected sinogram are, respectively, obtained. The two sinograms are fused into the fused sinogram. The fused sinogram, the original sinogram, and the high-density material sinogram are fused into the final sinogram. Finally, the filtered back projection reconstruction algorithm is used to reconstruct the final sinogram into the reconstructed CT image. The reconstructed CT image and high density material image are fused into the final image. The experimentation results show that the method proposed in the paper can obtain better correction effect than the classical correction methods in vision.

1. Introduction

CT imaging system is one of the radiography technologies, which is widely used in medical diagnosis, industry and security detection, and other fields. In the medical field, when the CT imaging system moves around the body, the detector collects projection data. Then, these data are input into the computer, and the two-dimensional fault images or three-dimensional images are reconstructed and displayed with the help of computers. In normal case, the reconstructed CT image is clear. However, during the course of work, if the scanning area contains dental implant, internal fixture, and the high density material, such as prosthesis, the reconstructed CT image contains some streak artifacts with the collected projection data. There are some reasons that can lead to streak artifacts. In general, the causes can be summarized as beam hardening [1], partial volume effect [2], the noise and movement, etc. The streak artifacts in the CT image affect the resolution of CT image, reduce the CT image quality, and seriously affect the diagnosis effect of medical workers. Therefore, people think of a number of methods reducing the streak artifacts and raising the CT image qualities.

In general, these methods can be divided into two types, namely, interpolation-based correction method [3–8] and iterative-based correction method [9–12]. Interpolation-based correction method [3–8] obtains projection data of streak artifacts using the interpolation technique. The method mainly includes simple linear interpolation, polynomial interpolation, wavelet interpolation, etc. In recent years,

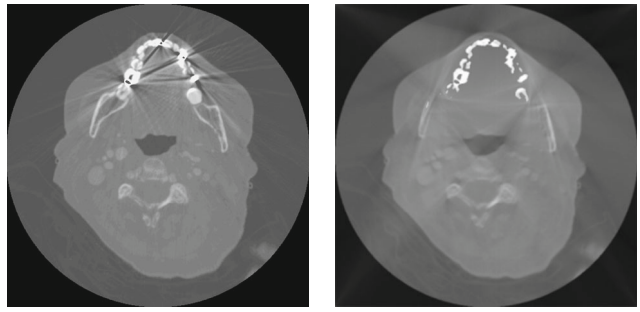

(a) (b)

Figure 1: Original CT image and corrected CT image.

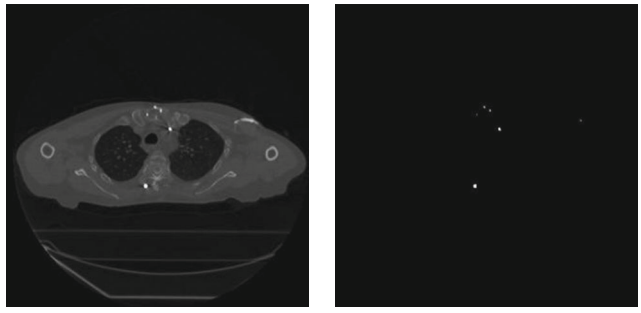

(a) (b)

Figure 2: The original CT image and segmented high density image.

people have proposed deep learning to correct metal artifacts in CT images, which also belongs to this type method. As can be seen from Figure 1, the secondary artifacts for the method are the key shortcomings. Iterative-based correction method mainly restores the streak artifact projection data by iterative method. Compared with the interpolation-based correction method [3–8], iterative-based correction method [9–12] can obtain better correction effect. But the low efficiency is fatal drawback for the method. During the work of the iterative-based correction method, it cost much time because the method restores the gray value of every position in the CT image by calculating.

2. Method

The correction method based on image segmentation and fusion CT image for streak artifacts is composed of the following five steps. To clearly show the every step and work process, the CT images collected in clinical data are used as experimentation data.

2.1. Multithreshold Segmentation and Sinogram Acquisition. Image segmentation is the basic technology for image processing, which is premise and method for the subsequent processing. Usually, the CT image contains multiple high density materials, which result in streak artifacts in reconstructed CT image. Therefore, to optimally segment these high density materials from CT image, the multithreshold values are used to segment CT image. The threshold acquisition adopts Otsu algorithm.

Here, Otsu algorithm is extended to multithreshold CT image segmentation. The algorithm utilizes N threshold segment the CT image into $N+1$ classes. The following formula (1) is variance between $N+1$ classes [13].

$$\begin{aligned} D(t_1, t_2, \cdots, t_n) = {} & \omega_0\omega_1(\mu_0 - \mu_1)^2 \\ & + \omega_0\omega_2(\mu_0 - \mu_2)^2 + \cdots + \omega_0\omega_n(\mu_0 - \mu_n)^2 \\ & + \omega_1\omega_2(\mu_1 - \mu_2)^2 + \omega_1\omega_3(\mu_1 - \mu_3)^2 \\ & + \cdots + \omega_{n-1}\omega_n(\mu_{n-1} - \mu_n)^2, \end{aligned} \tag{1}$$

$$\begin{aligned} & \omega_{k-1} = \textstyle\sum_{i=t_{k-1}+1}^{t_k} p_i, \\ & \mu_{k-1} = \textstyle\sum_{i=t_{k-1}+1}^{t_k} (ip_i/\omega_{k-1}), \\ & k \in [1, n+1]. \end{aligned}$$

The optimal segmentation threshold $0 \le t_1 \le t_2 \cdots \le t_n \le L-1$ uses the biggest of $D(t_1, t_2, \cdots, t_n)$ for $n+1$ the total variance between the classes, namely, $(t_1, t_2, \cdots, t_n) = \arg\max\{D(t_1, t_2, \cdots, t_n)\}$.

The original CT image is segmented into the high density image and no-high density image. Figure 2 shows the original CT image and high density material image.

2.2. Linear Interpolation Correction and Mean Filter. The original CT image and high density material image are projected into the original sinogram and high density material sinogram, respectively. After obtaining the original CT image, the high density material image, and their corresponding sinograms, the simple linear interpolation is used

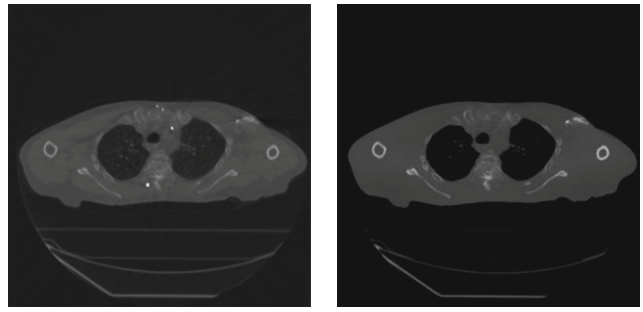

(a) (b)

Figure 3: Corrected CT image and filtered CT image.

to correct the original CT image, such as Figure 3(a). As can be seen from Figure 3(a), the secondary artifacts are shown in the corrected CT image. The secondary artifacts seriously affect the clarity for the CT image edge structure. To preserve the CT image edge structure, during the course of experimentation, the mean filter applied in the corrected CT image.

There are M rows and N columns for the corrected CT image. The $v(i,j)$ is the grey value for coordinate pair (i,j). $g(i+m,j+n)$ is defined as follows:

$$g(i+m,j+n)=\begin{cases} v(i+m,j+n) & |v(i+m,j+n)-v(i,j)|\le T \\ 0 & |v(i+m,j+n)-v(i,j)|>T \end{cases}. \tag{2}$$

Here, $-k\le m\le k$ and $-k\le n\le k$ (k for the size of the neighborhood). The $v(i+m,j+n)$ is the grey value for coordinate pair $(i+m,j+n)$. T is the threshold. During the course of the experimentation, it is necessary to choose the appropriate value T, which is too small to remove the secondary artifacts. On the contrary, if the value T is too big, the CT image edges are blurred. Generally speaking, the organization structure in CT image is composed of soft tissue, bone tissue, and air. The difference between them is 350 HU. To preserve the organization structure edge for CT image, the threshold T equals to 350.

The following (3) is mean filter formula for the corrected CT image.

$$R(i,j)=\frac{\sum_{m=-k}^{k}\sum_{n=-k}^{k}g(i+m,j+n)}{C}. \tag{3}$$

Here, C is the number of elements around (i,j). R and $R(i,j)$, respectively, denote the filtered image and grey value for coordinate pair (i,j). Figure 3(b) shows the filtered image.

As can be seen from Figure 3(b), the filtered image is very clear. But the high density material is removed from the filtered CT image. Therefore, the filtered CT image must be further dealt.

2.3. Image Fusion. After the corrected CT image is filtered, the image is projected into the filtered sinogram. According to the locations of the high density material sinogram (Figure 4(a)) in the original CT image sinogram (Figure 4 (b)) and filtered sinogram (Figure 4(c)), the high density material sinogram in the original CT image (Figure 4(d)) and high density material sinogram in filtered image sinogram (Figure 4(e)) are obtained. According to a certain proportion, the high density material sinogram in the original CT image and filtered image sinogram are fused into fusion sinogram. In the same way, the fusion sinogram (Figure 4 (f)), the original sinogram and the high density material sinogram with a certain proportion are fused into the final sinogram (Figure 4(g)). Figure 4 shows the corresponding images for above every step.

2.4. Projection Reconstruction and High Density Image Fusion. In practice, the filtered back-projection reconstruction algorithm is used to reconstruct the final sinogram into the corrected CT image. Figure 5(a) shows the corrected CT image with the final sinogram. As can be seen from Figure 5(a), the streak artifacts were reduced from the original CT. But the high density materials disappear from the corrected CT image. The reason for the phenomenon is that the corresponding sinogram for high density materials is not included in the final sinogram. To show the high density materials in the corrected image, the corrected CT image and high density material image are fused with the ratio 0.5 : 0.5. The final corrected image can be seen from Figure 5(b).

3. Experimentation Data Acquisition

To further evaluate and demonstrate the performance of the streak metal artifact reduction method based on sinogram fusion and tissue-class model in CT images, providing the above clinical CT image, the other clinical CT images are provided in the selection.

The proposed F-MAR method is tested in several clinical cases. They are grouped into two sets, as presented in Figures 3 and 4. In Figure 3, every case only contains a metal object. The other has at least two metal objects in the clinical cases in Figure 4. These images with the extension ".dcm" are downloaded from the web site http://www.revisionrads.com of REVISION RADIOLOGY group. In Figure 3, Figure 3(a1) and Figure 3(b1) are two patients with two deep brain stimulators. The patient with Figure 3(c1) has a metallic dental filling, while the head CT images with a cerebral artery aneurysm are shown in

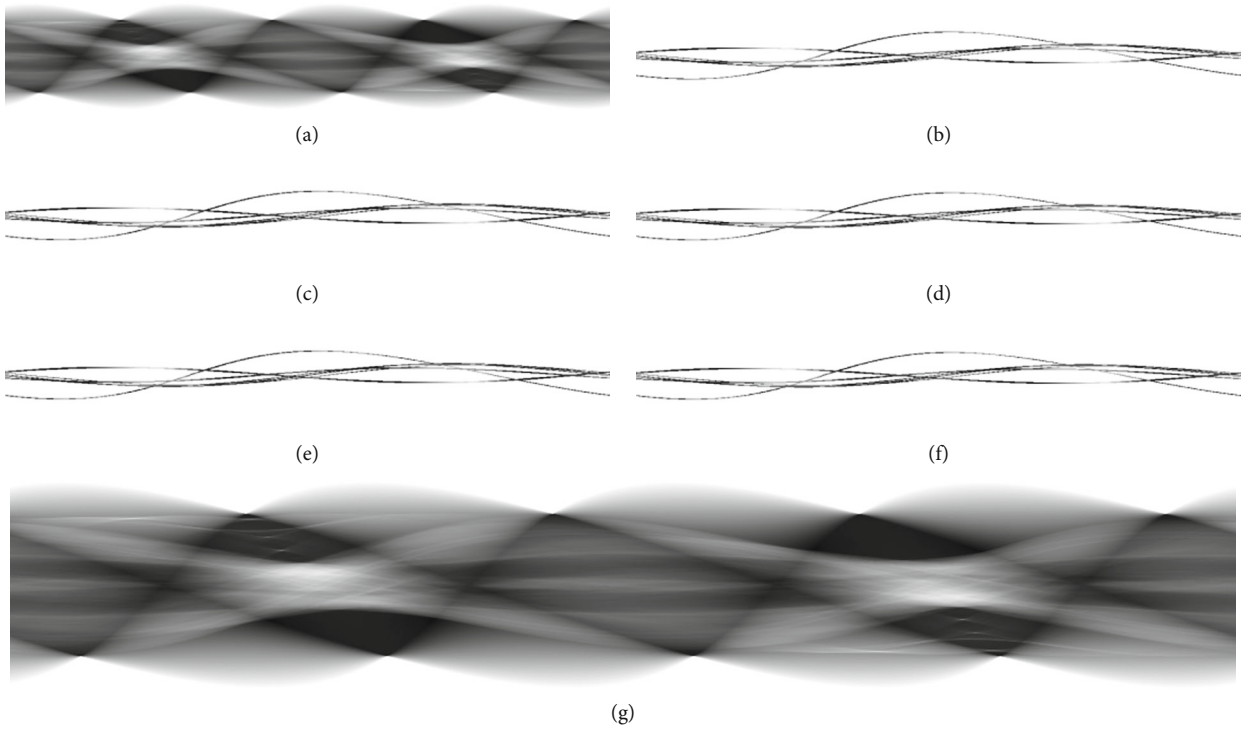

(a) (b) (c) (d) (e) (f) (g)

Figure 4: (a) Original CT image sinogram. (b) High density material sinogram. (c) Filtered image sinogram. (d) The high density material sinogram in the original CT image. (e) The high density material sinogram in filtered image sinogram. (f) Fusion sinogram. (g) Final sinogram.

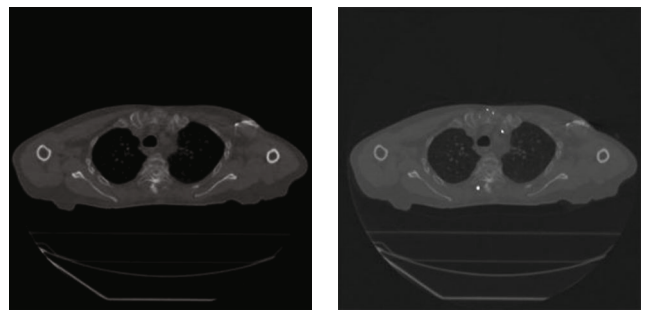

(a) (b)

Figure 5: Corrected CT image and fused CT image.

Figure 3(d1). Figure 3(e1) is a patient with unilateral hip prostheses. Compared to the Figure 3, the metal artifacts of the four cases in Figure 4 are caused from pedicle screw (Figure 4(a1)), bilateral hip prostheses (Figure 4(b1)), a cerebral artery aneurysm (Figure 4(c1)) and unilateral hip prostheses (Figure 4(d1)).

4. Results

In this paper, the linear interpolation MAR method, polynomial interpolation MAR method, and proposed MAR method are shortened as L-MAR, P-MAR, and F-MAR. The all corrected results with L-MAR, P-MAR, and F-MAR are presented in the section.

The results for the clinical data sets are shown in Figures 6 and 7. In Figure 6, Figures 6(a1), 6(b1), 6(c1), 6(d1), and 6(e1) are the original images. As can been from the images, the cases contained a lot of streak metal artifacts emanating from the metal object. Compared to the original images, the streak metal artifacts have been greatly reduced by using the L-MAR method. But the new artifacts are introduced in the corrected cases. As be shown in Figures 6(a2)–6(e2)). The P-MAR method has almost the same correction effects with the L-MAR method. Their corrected results with P-MAR method are provided in Figures 6(a2)–6(e3). Images from Figures 6(a4)–6(e4) are the corrected results using the F-MAR method proposed in the paper. It is noteworthy that the presented approach greatly reduces the streak metal artifacts in the original images while not producing the new artifacts in the corrected images. For more complex structures (at least two objects with different size and type), the original cases

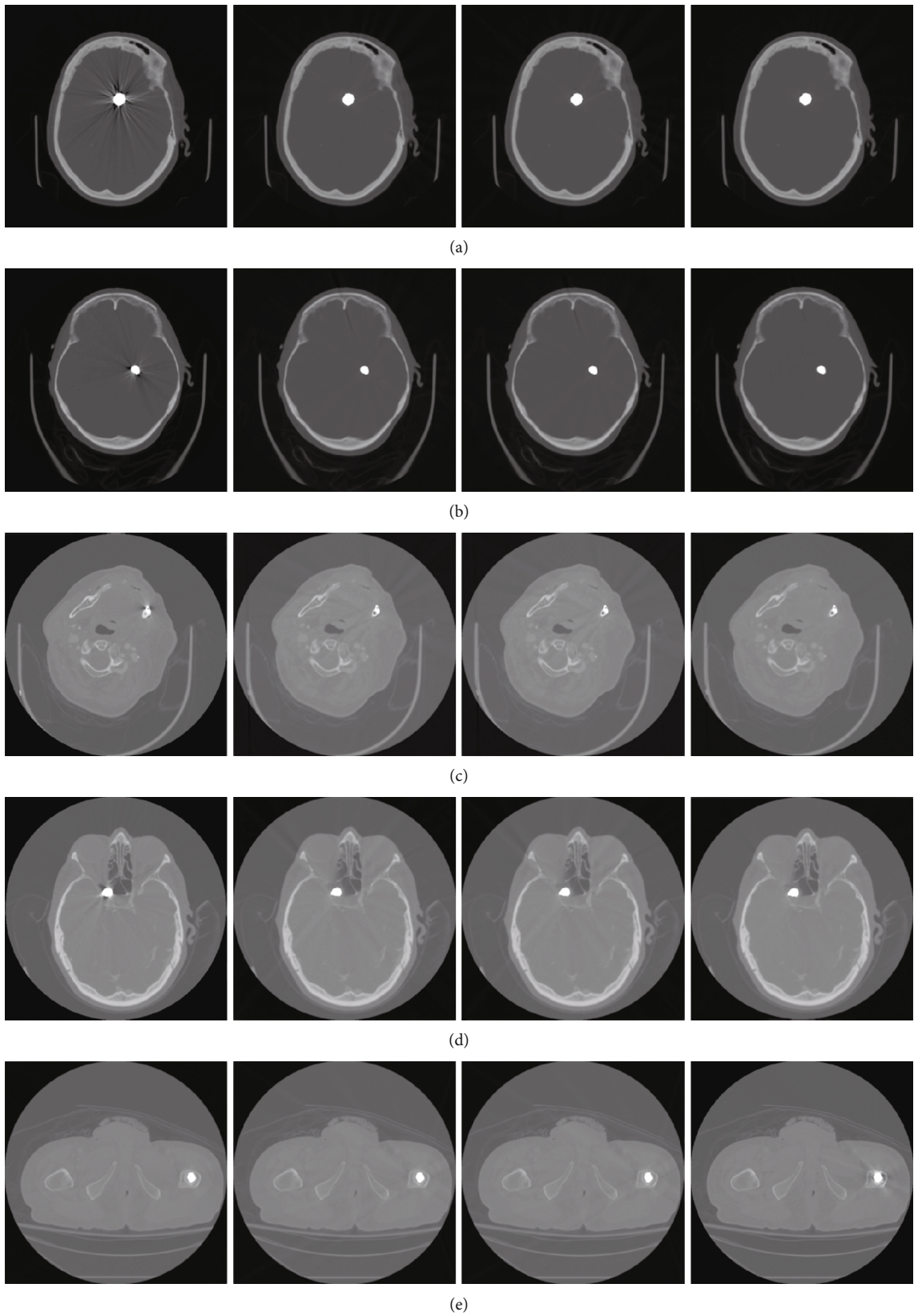

(a)

(b)

(c)

(d)

(e)

Figure 6: Streak metal artifact reduction in clinical cases with a metal object. Five sets of original and corrected results corresponding to (a–e). Each set successively contains the original, L-MAR, P-MAR, and F-MAR images. (a, b) Two patients with two deep brain stimulators. The patient with (c) has a metallic dental filling, while the head CT images with a cerebral artery aneurysm are shown in (d). (e) A patient with unilateral hip prostheses ($C = 500$ HU/$W = 1500$ HU).

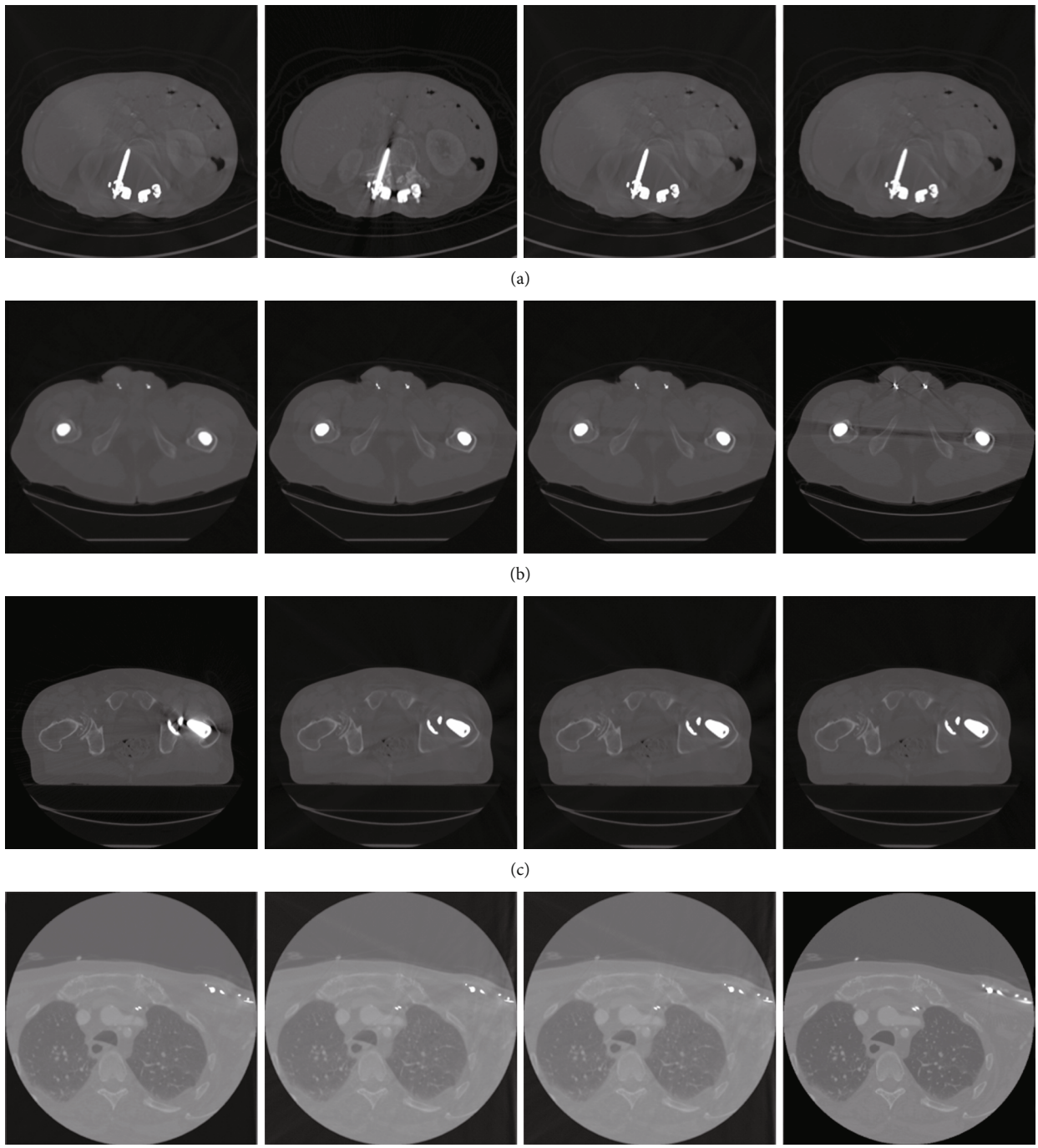

Figure 7: Streak metal artifact reduction in clinical cases with at least two metal objects. Five sets of original and corrected results corresponding to (a–e). Each set successively contains the original, L-MAR, P-MAR, and F-MAR images. The metal artifacts of the five cases are caused from pedicle screw (a1–a4), bilateral hip prostheses (b1–b4), a cerebral artery aneurysm (c1–c4), and unilateral hip prostheses (d1–d4) ($C = 500$ HU/$W = 1500$ HU).

are shown in Figures 7(a1), 7(b1), 7(c1), and 7(d1). Obviously, these images are blurred by the metal objects in the cases. Images from Figures 7(a2)–7(d2) are the results with the L-MAR method. The corrected results with P-MAR method are provided in Figures 7(a3)–7(d3). It is very obvious that the L-MAR and P-MAR methods can reduce the streak metal artifacts, and the new artifacts still appear in the corrected results. The best correction approach is the proposed F-MAR method in this paper, and its correction results are shown in Figures 7(a4)–7(d4)).

5. Discussions

The streak metal artifacts arising from metal object degrade even deteriorate CT images quality and impact the clinical diagnosis effect of the medical workers. Therefore, the researchers propose several methods to reduce the streak metal artifacts in the CT images. In these methods, the L-MAR method and its corresponding variation, namely, P-MAR methods, are the simplest and most efficient approach. On the whole, they can effectively reduce the streak metal artifacts in the images and improve the quality of the images. However, the new artifacts appearing in corrected images are the main drawback. The basic problem of the phenomenon is that the interpolation-based method loses the relevant information during the interpolation. To solve the problem, in the work, the F-MAR method is proposed to reduce the metal artifact reduction in CT images. The aim of the approach is to restore that the lost data after the interpolation method is used. To restore the lost data, the F-MAR method fuses the corresponding position original metal object sinogram, smoothed sinogram, and metal object sinogram. In the corresponding position, original metal object sinogram contains the lost information during the interpolation (about its details have been introduced above).

In clinical case studies, experiments show that the F-MAR method obtains best results among the L-MAR method, P-MAR method, and F-MAR method. These experimental results also further verify that the proposed method is superior to the traditional classical method.

6. Conclusion

The streak artifacts in CT image have been one of the key factors that affect on the CT image qualities. These streak artifacts not only obscure the CT image but also affect the diagnosis effect of the disease and even the further development of CT imaging system. To solve the problem and improve the image quality, the researchers propose a variety of approaches. On the basis of analyzing the classical streak artifact correction, the paper proposes the streak artifact correction based on multithreshold segmentation and image fusion and compares the method with classical correction methods. The experimentation results indicate that both comparison from the aspects of visual effect and streak artifact reduction, the method proposed in the paper can obtain better effect. This will lay a solid foundation for further research and clinical application in the future.

Data Availability

The data used to support the findings of this study are available from the corresponding author upon request.

Conflicts of Interest

The authors do not have any possible conflicts of interest.

Acknowledgments

The work is supported by the National Natural Science Foundation of China (No. 2017YFC0107900), the Scientific Research Foundation of Education Department of Anhui Province (No. KJ2018A0431), the Study Project for Excellent Youth Backbone Talents in Universities at Home and Abroad (No. gxgwfx2018077), and the research initiation fund project of Chuzhou University (No. 2020qd15).

References

[1] F. Esmaeili, M. Johari, and P. Haddadi, "Beam hardening artifacts by dental implants: comparison of cone-beam and 64-slice computed tomography scanners," *Dental Research Journal*, vol. 10, no. 3, pp. 376–381, 2013.

[2] G. J. Bootsma, F. Verhaegen, and D. Jaffray, "The effects of compensator and imaging geometry on the distribution of X-ray scatter in CBCT," *Medical Physics*, vol. 38, no. 2, pp. 897–914, 2011.

[3] P. M. Queiroz, F. C. Groppo, M. L. Oliveira, F. Haiter-Neto, and D. Q. Freitas, "Evaluation of the efficacy of a metal artifact reduction algorithm in different cone beam computed tomography scanning parameters," *Oral Surgery, Oral Medicine, Oral Pathology, and Oral Radiology*, vol. 123, no. 6, pp. 729–734, 2017.

[4] S. O. Jin, J. G. Kim, S. Y. Lee, and O.-K. Kwon, "Bone-induced streak artifact suppression in sparse-view CT image reconstruction," *Bio Medical Engineering OnLine*, vol. 11, p. 44, 2012.

[5] L. Yuanjin, C. Yang, L. Limin, P. Zhang, and Q. Zhang, "Fast CT metal artefacts correction based on derivative and region-based filling," *Journal of Medical Imaging and Radiation Oncology*, vol. 55, no. 6, pp. 535–541, 2011.

[6] N. S. Paul, J. Blobel, E. Prezelj et al., "The reduction of image noise and streak artifact in the thoracic inlet during low dose and ultra-low dose thoracic CT," *Physics in Medicine and Biology*, vol. 55, no. 5, pp. 1363–1380, 2010.

[7] J. Kim, H. Nam, and R. Lee, "Development of a new metal artifact reduction algorithm by using an edge preserving method for CBCT imaging," *Journal of the Korean Physical Society*, vol. 67, no. 1, pp. 180–188, 2015.

[8] Z. S. Ying, T. Bae Kyongtae, W. Bruce et al., "A wavelet method for metal artifact reduction with multiple metallic objects in the field of view. X-ray," *Science and Technology*, vol. 10, pp. 67–76, 2002.

[9] W. Wuest, M. S. May, M. Brand et al., "Improved image quality in head and neck CT using a 3D iterative approach to reduce metal artifact," *American Journal of Neuroradiology*, vol. 36, no. 10, pp. 1988–1993, 2015.

[10] J. Aissa, C. Thomas, L. M. Sawicki et al., "Iterative metal artefact reduction in CT: can dedicated algorithms improve image quality after spinal instrumentation?," *Clinical Radiology*, vol. 72, no. 5, pp. 428.e7–428.e12, 2017.

[11] J. Dong, S. Kannenberg, and C. Kober, "Metal-induced streak artifact reduction using iterative reconstruction algorithms in X-ray computed tomography image of the dent alveolar region," *Oral Surgery, Oral Medicine, Oral Pathology, and Oral Radiology*, vol. 115, no. 2, pp. 63–73, 2013.

[12] A. Kondo, Y. Hayakawa, J. Dong, and A. Honda, "Iterative correction applied to streak artifact reduction in an X-ray computed tomography image of the dento-alveolar region," *Oral Radiology*, vol. 26, no. 1, pp. 61–65, 2010.

[13] N. Otsu, "A threshold selection method from gray-level histograms," *IEEE Transactions on Systems, Man, and Cybernetics*, vol. 9, no. 1, pp. 62–66, 1979.